ALUMINIUM FLUORIDE CONSUMPTION AND CONTROL IN SMELTING CELLS

Invited lecture for presentation by Barry Welch at 6th Molten Slags, Fluxes and Salts Conference,
Stockholm, 12-16 June 2000
Co-authored by
M.M. Hyland, E.C. Patterson, F. Stevens-McFadden & B.J. Welch

High Temperature Materials and Processing Group
The University of Auckland
New Zealand

ABSTRACT

For optimum operation and performance of aluminium smelting cells, each technology has an optimum aluminium fluoride concentration for the solvent electrolyte. The actual value used is influenced by the alumina dissolution and differs because of different alumina feeding technologies.

The aluminium fluoride is consumed within the cell and therefore, chemical analysis is performed as part of the process to determine the amount required for replenishment of the consumption. However the cell has a dynamic energy balance and that causes simultaneous variations in the distribution of solid and liquid electrolyte components, complicating the overall situation. Ultimately, it results in the chemical analysis varying. Thus it becomes a major challenge to determine the amount of aluminium fluoride that needs to be added to replenish the consumption, whilst maintaining the cell at close to its optimum range.

In the first part of this paper, the consumption mechanisms are reviewed with respect to the process variability. In the second part the approach used to control the aluminium fluoride concentration is reviewed, and the impact of the energy dynamics is also analysed.

PART I: Consumption

INTRODUCTION to BATH CHEMISTRY and CONSUMPTION

It is well established that the cryolitic anion (AlF_6^{3-}) arising on melting cryolite (Na_3AlF_6) is essential for dissolving alumina for the electrolytic production of aluminium. In practice the cryolite also dissociates on melting to give an equilibrium concentration of the cryolitic species, sodium fluoride and sodium tetrafluoroaluminate according to equation 1:

$$Na_3AlF_6 \;\rightleftharpoons\; 2NaF + NaAlF_4 \qquad\qquad\text{- (1)}$$

Since this melt also dissolves metal, leading to a lowering in current efficiency, it has been shown that it is desirable to not only lower its melting point, but also to increase the concentration of the sodium tetrafluoroaluminate. Essentially the dissolving reaction on adding aluminium fluoride can be given by the following reaction:

$$Na_3AlF_6 + 2AlF_3 \;\rightarrow\; 3NaAlF_4 \qquad\qquad\text{- (2)}$$

This also lowers the melting point. The other additive commonly used is calcium fluoride. Its presence has little impact on the concentration of the dissolving cryolitic anions, whilst lowering the melting point significantly.

1

The addition of any species has an impact on both the saturation solubility of alumina added to the cells, and the speed with which undissolved alumina can dissolve in the liquid melt. While having good alumina feeding systems can minimize this impact, inevitably the occasional undissolved alumina slurry is formed. Here some of the undissolved alumina settles beneath the metal pad encompassed in a fluoride electrolyte phase that is of different composition and melting point from the bulk electrolyte. This composition difference results from phase segregation and sodium transport through the slurry.

Practically, severe alumina solubility problems are encountered with all feeding systems if the superheat of the electrolyte is below 5°C. Conversely, whilst above 15°C superheat the
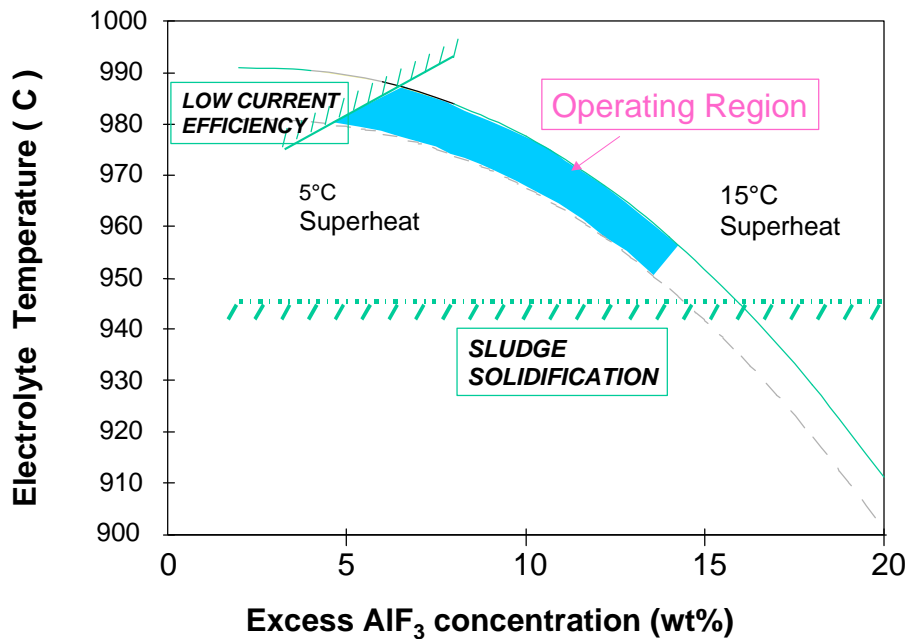

Figure1: Restrictions on Electrolyte Operating Conditions (Taylor, 1997)

protective side ledge melts. Accordingly there are operating restraints on the range of electrolyte solvent compositions and temperatures that can be used (as illustrated in figure 1). Note that Figure 1 is for a 3 wt% alumina concentration. Since the control system necessitates cycling of dissolved alumina concentration - typically varying between 2 and 3% - this cycling has a second impact on the cell temperature at fixed superheat, but not on the sludge freezing point.

Aluminium fluoride concentrations in the electrolyte can vary from two main sources:

• Variations in distribution of the fluoride materials in the cell (see Figure 2).
• Losses of the aluminium fluoride that do not balance the addition rate.

There are a number of causes for the change in heat balance that leads to the change in distribution of the fluoride components in the cell. The primary driver in this change is the superheat of the electrolyte, which will cause a melting or freezing of the side ledge. Accumulation of sludge is another cause.
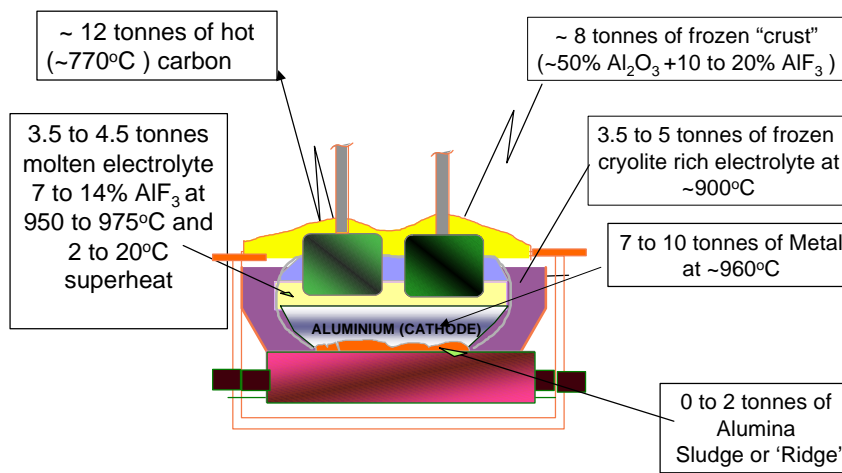
Figure 2: Materials distribution in a 150 to 200 kA cell (Welch, 1998).

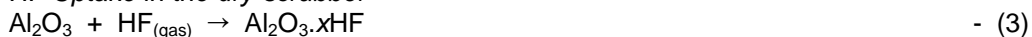**THE CONSUMPTION OF ALUMINIUM FLUORIDE**

There are six processes that contribute to the consumption of the aluminium fluoride added to the cells. These are:
- Reacting with the sodium oxide content of the alumina fed to the cell (which typically ranges between 0.25 and 0.5 wt%).
- Reacting with the calcium oxide component of the smelter grade alumina (which typically ranges from 0.015 to 0.04 wt%).
- Transpiration losses through vaporisation of the volatile sodium tetra fluoraluminate.
- Electrochemical oxidation from the anode hydrogen (which typically has a concentration of about 0.05 wt%) to form gaseous hydrogen fluoride.
- Hydrolysis of the electrolyte by water introduced through either
    - Humid air passing over the electrolyte surface,
    - Water adsorbed on the surface of the alumina during storage or dry scrubbing,
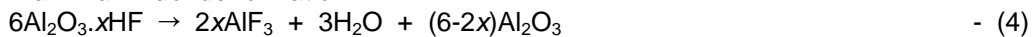   - Crystalline water that has not been previously decomposed.

The aluminium fluoride balance is also impacted by sodium uptake in the cathode. In this case it results in it being a source of aluminium fluoride.

Another input source for AlF_3 is recycled materials when dry scrubbing systems are used in the overall smelting process. Most commonly smelters use dry scrubbers which adsorb gaseous hydrogen fluoride on the surface of primary (unreacted) alumina. This is subsequently recycled back to the cell as aluminium fluoride (and some bath particulate, combined in the form of secondary alumina), according to the following two reactions:

HF Uptake in the dry-scrubber
$$Al_2O_3 + HF_{(gas)} \rightarrow Al_2O_3.xHF \hspace{3cm} - (3)$$

Aluminium fluoride formation
$$6Al_2O_3.xHF \rightarrow 2xAlF_3 + 3H_2O + (6-2x)Al_2O_3 \hspace{2cm} - (4)$$

Besides the recycled aluminium fluoride, the condensed vapours are usually entrapped and recycled with them. However, since the vapours often have impurities associated with them, the same material is not necessarily always returned to all cells. Thus an overall plant balance will result in more than 99% of the vapours and gaseous components being recycled, although this is not the case for individual cells or potlines that are managed differently. The problem is aggravated by segregation.

The Impact of Cathode Sodium Uptake
This is greatest in the early operating life of the cell, but continues throughout its operating life due to the temperature gradient down the cathode block. In some failed cells of very high age, liquid sodium is sometimes found condensed on the collector bar underneath the cathode blocks.
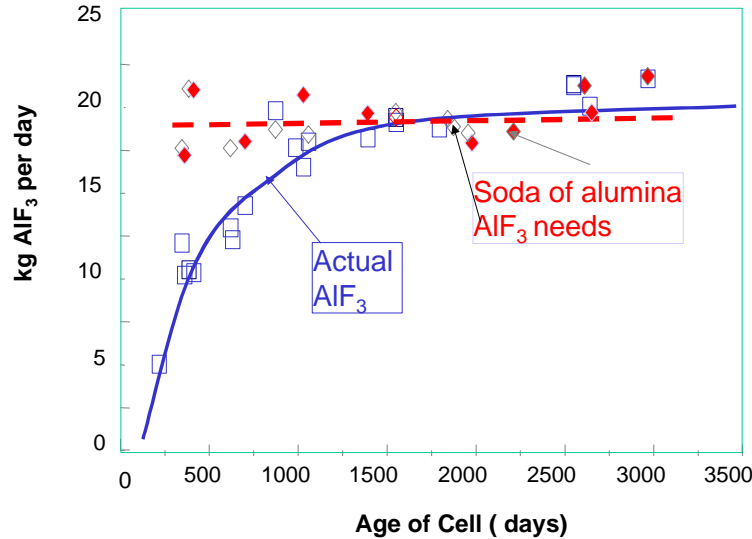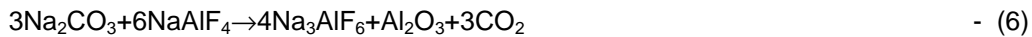

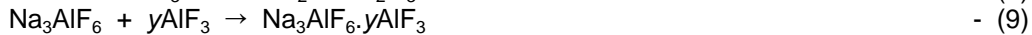**Figure 3: History of AlF$_3$ added to a cell (30 day averages).**

For mature cells (greater than 1200 days) the aluminium fluoride consumption approximates that predicted from the sodium oxide and calcium oxide contents when the cells are fitted with dry scrubbers and completely recycled. The difference indicates that the continuing sodium uptake is of small value and less than 1% of the overall consumption. This is illustrated in figure 3, where each data point represents 30-day averages.
The reduced AlF$_3$ demand in the first 1000 days is a consequence of the cathode uptake of Na, since all other losses are accounted for. The data shows that in the first months it is necessary to add Na$_2$CO$_3$ to compensate for the large amount of Na entering the cathode, according to the following overall reaction:

$$4Na_3AlF_6 + 3C_{(anode)} + Al_2O_3 + 6xC_{(cathode)} \rightarrow 6NaAlF_4 + 3CO_2 + 6NaC_x \qquad - (5)$$

$$3Na_2CO_3 + 6NaAlF_4 \rightarrow 4Na_3AlF_6 + Al_2O_3 + 3CO_2 \qquad - (6)$$

Aluminium Fluoride required for the Oxide Impurities of Alumina
Metals oxides that are reduced by the aluminium do not contribute to the net aluminium fluoride consumption, even though their dissolution reaction may involve forming a fluoride. The amount required for reaction can be predicted from the concentration of the impurities in the oxides, according to the following reactions (equations 7 to 9). It should be noted that since smelters work to a chemical analysis, one needs to add an excess amount of aluminium fluoride in order to adjust the concentration of the newly formed cryolite to that of the bulk melt.

$$3Na_2O + 4AlF_3 \rightarrow 2Na_3AlF_6 + Al_2O_3 \qquad - (7)$$
$$3CaO + 2AlF_3 \rightarrow 3CaF_2 + Al_2O_3 \qquad - (8)$$
$$Na_3AlF_6 + yAlF_3 \rightarrow Na_3AlF_6.yAlF_3 \qquad - (9)$$

where y is the proportion of excess AlF$_3$ based on its target concentration.

4

Simply based on a material balance of the raw material - since 1.9 tonnes of alumina are required per tonne of aluminium - the aluminium fluoride required for these reactions can be given by the following relationships:

$$\text{kg AlF}_3/\text{tonne Al} = 34.3\,[\%Na_2O] + 19\,[\%CaO] + 0.49\,[\%Na_2O][\,X_{AlF_3}\,] \qquad - (10)$$

where % Na$_2$O and % CaO are the weight percentages of the oxides in the primary alumina and X is the target AlF$_3$ concentration in the electrolyte.

In the long term, this is actually obeyed, as is seen from the leveling out of the data presented in Figure 3. The only other contribution to aluminium fluoride consumption for the mature cells is fugitive emissions, and these are typically less than 1%.

Vaporisation Losses of Aluminium Fluoride
This can be predicted by assuming the anode gases formed leave the electrolyte saturated in the vapour. Accurate vapour pressure equations have been published by Kvande (1993) and co-workers, enabling predictions. However, such a prediction only gives the maximum amount since it assumes that all this material leaves the cell. In reality, a high proportion can permeates through the crust and cover. The fraction that is retained in the crust is therefore technology-dependent and generally unknown. It can, however, be predicted from the sodium and fluorine analysis of the secondary alumina. This prediction is useful, but is complicated by the difficulty in sampling from the dry scrubber product due to extensive segregation. For a centre break technology system, a typical increase in sodium content (over the base amount from the refinery) is 0.4 to 0.6 wt%. However, the net loss is less since the particulates contribute to the above figure. This corresponds to a gross aluminium fluoride loss of 4 to 6 kg/tonne Al which compares to predicted values from complete vaporization of 5 to 7 kg/tonne Al via vapourisation for an electrolyte containing 10 wt% excess AlF$_3$. The vapourisation values were calculated using components of Haupin and Kvandes' (1993) mathematical model for bath vapourisation. Variation in the value result from differences in bath coverage, which with better integrity increasingly scrubs the emissions. The vaporization prediction is a maximum as discussed earlier.

It is established that the vapours tend to disproportionate to chiolite (Na$_5$Al$_3$F$_{14}$) and aluminium fluoride. It has also been suggested these species undergo hydrolysis reactions forming more hydrogen fluoride. The extent to which this reaction occurs is questionable since the hydrolyzing water would come from the air sucked over the cell by the fumes capture system. That air does not exceed 150°C, whereas the hydrolysis reaction requires temperatures in excess of 600°C according to thermodynamic data presented in figure 4. Whether or not this reaction occurs is irrelevant to the aluminium fluoride loss, since the hydrolysis product would be adsorbed on the alumina and recycled.
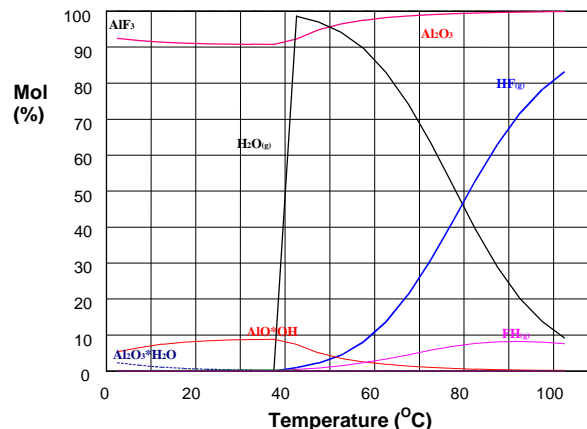

Figure 4: Thermodynamic prediction of the temperature region for hydrolysis of AlF$_3$.

Losses due to the Hydrogen of the Anode
In a comprehensive early study, which involved electrolyte containing less aluminium fluoride, Henry (1968) suggested that a high proportion of the hydrogen of the anode was converted to gaseous hydrogen fluoride. The typical hydrogen contents of anodes range between 0.04 and 0.08wt%. If one takes into account only the carbon consumed being electrolytically (approximately 360 kg per tonne of aluminium) the consumption of aluminium fluoride would be given by the relationship:

$$AlF_3 \text{ Consumed/tonne Al } = 98 \times [wt\% \ H_2 \text{ in anode}]. \qquad - (11)$$

Thus for a typical cell this would contribute approximately 5 kg of aluminium fluoride per tonne of aluminium produced. However, this has been an area of study that has been overlooked until recently and confirmation of the amount in the open literature is still awaited.

Measurement of Aluminium Fluoride Lost through Hydrolysis of Bath
With the recent development of sensitive infrared instrumentation, measuring the hydrogen fluoride content in the duct has become feasible. This enables the total gaseous hydrogen fluoride at any point in the system to be measured. The total gaseous hydrogen fluoride includes the contributions from the anode and any hydrolysis of the vapours, as discussed above. Thus it is not a direct measure. However, the measure does give a limit to the amount. In Figure 5, we see that the hydrolysis reaction tends to increase with the excess aluminium fluoride concentration in the electrolyte. This data represents potline or plant average for a bar-break operating cell that was only fed with primary alumina, but had secondary dust filters that recycled the particulate (vaporization) fluorides to the cell. Accordingly, it gives a direct measure of the increase in hydrogen fluoride emissions with excess aluminium fluoride. (The data has not been compensated for the consumption through the sodium oxide content of the alumina, but this was fairly constant in the range 0.25 to 0.3 wt% in this instance).
This suggests that the hydrolysis proceeds via the following reaction,

$$3NaAlF_4 + 3H_2O_{(g \text{ or diss})} \rightarrow Na_3AlF_6 + Al_2O_3 + 6HF_{(g)} \qquad - (12)$$
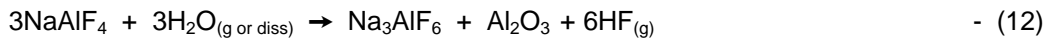
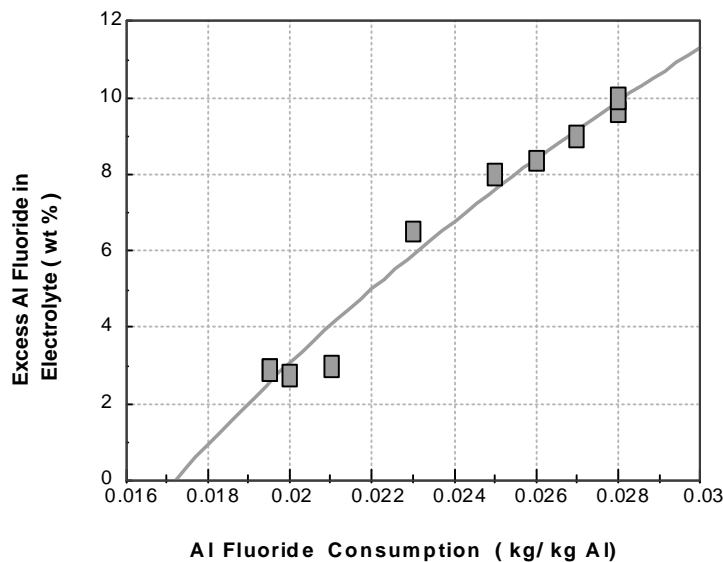and the rate of the reaction is dependent on the dissolved concentration of the aluminium fluoride.

Figure 5: Actual AlF$_3$ consumption for a given Excess AlF$_3$ wt %

It does not, however, differentiate through the various forms of the hydrolysing water that is introduced with the alumina. The forms of the hydrolyzing water have already been noted (Hyland *et al* (2000)) and include:

- Water adsorbed on the alumina, but introduced to the cell through inadequate pre-heating. (This is likely to be a gaseous reactant as it evolves, with a finite residence time.)
- Crystalline water from the incomplete calcination of the alumina. It is known that water has a finite solubility in the electrolyte, and this probably arises from the crystalline water. (The solubility has been well established because of the production of hydrogen in the metal – a quality control concern for metal fabrication.) Whilst no data exists on the solubility of the water, it is reasonable to expect that this will be proportional or linked to the alumina concentration, and also the amount of crystalline water in the alumina.
- The vapours evolved from the cells (as discussed above) can also undergo hydrolysis with the water evolved in the zone immediately above the electrolyte. However, as Figure 4 demonstrates, there is only a finite temperature window for this hydrolysis reaction to occur.
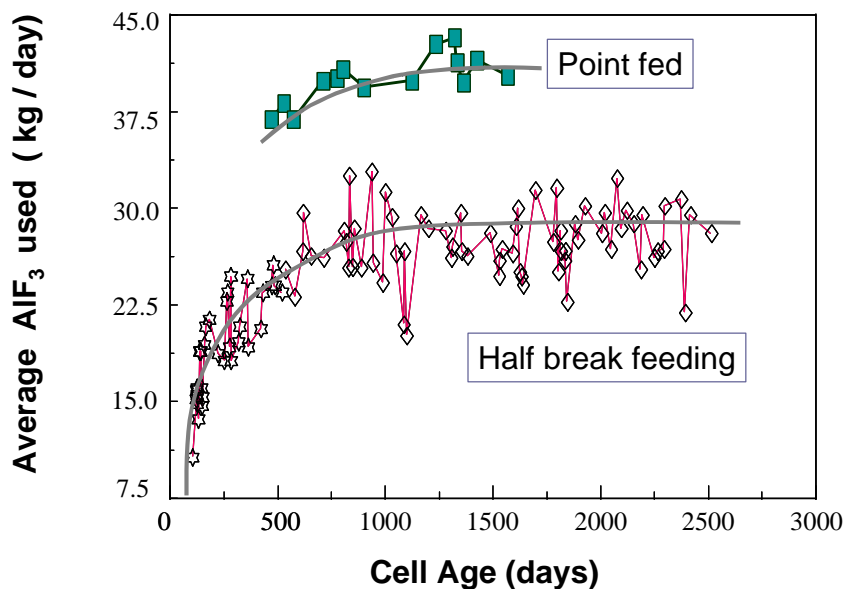

Figure 6: Comparing AlF$_3$ usage for a given feeder type on a potline.

The data of Figure 5 demonstrates that the amount of hydrolysis from the three potential contributors is fairly uniform over the long term but does not enable the relative concentrations to be determined.

Plant data also suggests that the hydrolysis reaction is also strongly influenced by the feeding methodology. Figure 6 compares daily aluminium fluoride consumption for a potline that had both point-feed and half centre bar-break feed technologies. The feeding was with primary alumina. It is seen that the point-fed technology has a much greater AlF$_3$ consumption than bar break technology.

For bar break technology a large amount of alumina is dumped from the hoppers along the centre channel at any one time. The thermal heat demand of this ensures electrolyte with which it comes into contact freezes on its under surface. Consequently, most of the alumina dumped from the hopper forms a new crust. The feed interval for bar break technologies is usually at least 15 minutes and, typically up to one hour. Accordingly, in that time the alumina is pre-heated much more than in the hopper and will lose some adsorbed water.

This alumina is added to the electrolyte at the next break time, and will predominantly have water of a crystalline nature rather than the adsorbed water.

For point fed cells the alumina has not been pre-heated as much and, therefore, will introduce adsorbed water as well as crystalline water to the electrolyte on a feeding action. Furthermore, because it is a small addition (typically one to three kg, as compared to 30 -100 kg for bar break), it will disperse more readily and have greater interfacial area for the hydrolysis reaction. This gives a higher rate of release of hydrogen fluoride from the cells. However, it must be emphasized again that it is technology-dependent, being linked with not only the mass of the feed, but the ability to disperse, and whether or not the point feed hole remains open.

Taking the data of Figure 6 (which is associated with a daily production of approximately 1.3 tonnes of aluminium), and applying Equation 10, gives an indication that, for this technology, the amount of aluminium fluoride consumed by the overall hydrolysis reaction (including vapourisation) is 13 kg / tonne of aluminium for bar break and 24 kg / tonne of aluminium for the point fed technology.

Summary of Contributions to the Consumption

The total consumption can be summarized by the contributions from the various individual causes. These are as follows:

Table 1: Summary of AlF_3 (kg/tonne Al) consumption at the cell.

	Source	Contribution Min	Max	Explanation
BATH	Na_2O	10	20	Variations depend on the sourced alumina. Max and min values based on 14% and 7% excess AlF_3 respectively and the extreme oxide compositions noted previously in the text. Affected by feeding rate.
	CaO	0.3	1	
HYDROLYSIS	H(Anode)	3	9	Dependant on the hydrogen content in the anodes. Ranges taken as 0.03% to 0.1%. Given as a rough estimate as there is currently little data in open literature.
	H_2O(Crystalline)	3	6	Dependent on the crystalline water content of the alumina, feeding method, and alumina feeding rate.
	H_2O(Adsorbed)	0.2	2	Dependant on the preheating of the alumina (feeding method), and alumina feeding rate. Limited effect on emissions.
DUST	Vapourisation	5	10	Minimum taken for an excess AlF_3 content of 7wt% with good cover. Maximum taken for an excess AlF_3 content of 14wt% with limited cover. Values are dependent on bath chemistry, cell setpoints and bath cover integrity.

Dynamic variations in these contents however give an indication of expected changes in a set time period. Table 2 presents these per tonne of Al produced:

Table 2: Expected Dynamic Variations (kg/tonne Al) of consumption contributors.

Source	Variation Min	Max	Explanation
Oxides (Na_2O, CaO)	0	3	Long term variations mainly due to compositional differences in the feed alumina shipments. ±15% daily variations due to changes in alumina feeding composition from sludge back feeding, cover dissolution and different feeding rates.
H(Anode)	0	0.5	Daily variations due to anode change. For similarly baked anodes and over the total anodes in a cell, variations will be minimal.
H_2O(Crystalline)	1	3	Variations dependent on feeding scheme. In an under and over feeding scheme, only short term changes due to aluminas feeding rate. Longer term variations dependant on shipment alumina composition
H_2O(Adsorbed)	0	0.5	Dependant on the preheating of the alumina (feeding method), and alumina feeding rate. Longer-term changes arise from changes in environmental humidity.
Vapourisation	0	2	Dependant on cell condition, chemistry and crust integrity. Sharp changes seen from heat balance changes.

Ultimately most of the emissions (hydrolysis and dust) component is recycled back to the cell via the scrubbing system. Total losses to the mass balance result from the oxide reactions and fugitive emissions. Fugitive emissions which can vary from 0.5 to 1.2 kg AlF_3 / tonne Al depending on cell technologies and smelter practices.

CONCLUSIONS ON AlF$_3$ CONSUMPTION.

By considering all the possible consumption contributors, several broad generalizations can be made about the loss processes affecting the AlF$_3$ content of an aluminium smelting cell. Most importantly is that for the overall process (a cell and dry scrubbing unit), the major loss of aluminium fluoride can be attributed to reactions with the oxide impurities (Na$_2$O and CaO) introduced with the feed alumina. The hydrogen fluoride emission losses contribute to the dynamic variability of the content. But in the long term 99% of these losses are recycled back to the cell via the secondary alumina feed. Moreover, variations from these material sources are relatively small. Most fluctuations stem from changes in the alumina feeding methodology (as well as sludge and crust dissolution), as this affects both hydrogen fluoride generation and the instantaneous amount of oxide impurities entering the cell. The hydrogen content of the anodes is a constant consumer of AlF$_3$, in the form of fluoride emissions. However this content also causes only minor dynamic variability in the AlF$_3$ content and is recycled as part of the secondary alumina feed. Therefore any large variations in the aluminium fluoride content is likely to be attributed to changes in the heat balance of the cell.

PART 2: Variability and Control

BACKGROUND TO VARIABILITY AND CONTROL

The analysis of the consumption of aluminium fluoride in smelting cells demonstrates that the changes in aluminium fluoride demand would normally be small, unless there is a major shift in one or more of:

- the sodium and impurity analysis of the primary alumina,
- the adsorbed or crystalline water of the alumina
- or the amount of alumina fed to a cell,
or the cover of the cell also changes dramatically.

Based on the normal daily production and the large liquid volume of electrolyte, one would not expect to see a major change in the aluminium fluoride material balance and hence concentration at constant bath volume. Practically however, as demonstrated in Figure 7, the change that occurs in a smelter is much more dramatic. While it is commonly assumed that the liquid bath volume is constant, it is known to change with heat balance. Process operators are in a dilemma – should they attempt to maintain constant concentration (because of its impact on current efficiency), or should they attempt to maintain the material balance, so that the concentration is correct when the cell is within its design mass and energy balance?]

Aluminium smelting cells are designed for a specific heat balance, and the resultant outputs for a cell operating within its design specifications are the superheat of the electrolyte(which is typically about 10°C) and side ledge thickness. These design outputs are based on the average energy demand of the inputs and outputs, coupled with the design heat losses.

Because the process has several batch operations superimposed on the continuous electrolysis, there is often a mismatch between the process energy requirements and the average energy balance for the process design. As seen in Figure 8, the process energy demand exceeds the design criteria whenever a new anode is introduced. The additions of alumina also increase the process energy demand, although there is a compensating energy flow as the alumina is electrolytically removed. Extra energy may be made available by:
- applying extra voltage (including noisy cell voltage),
- a significant transient surplus whenever the cell gets depleted of alumina and has an anode effect.
Further complications to the energy balance situation includes
- non-scheduled anode changes, which adds further to the process demand, and
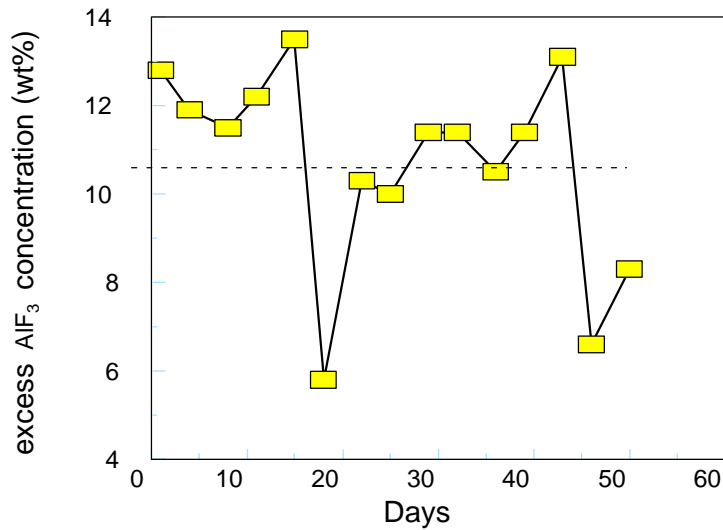- the changed heat flow as a consequence of metal tapping.

Figure 7: Variability over time in %excess AlF$_3$ in a Smelting Cell

The time scale over which some of the process energy demands and their consequences occur varies, in some instances being of the order of less than an hour but in other instances they can exceed a day. Whenever there is an energy imbalance within the electrolyte zone, there is invariably a shift in temperature as the energy surplus/deficit is accumulated initially as sensible heat. The more important consequence of the shift in bath temperature is a similar shift in the process superheat. Change in superheat is the driving force for the change in energy flow from the cell through the sidewall; hence the ledge covered sidewall is the main heat valve in an operating smelting cell and the consequence of changes in heat flow is melting or freezing of ledge.
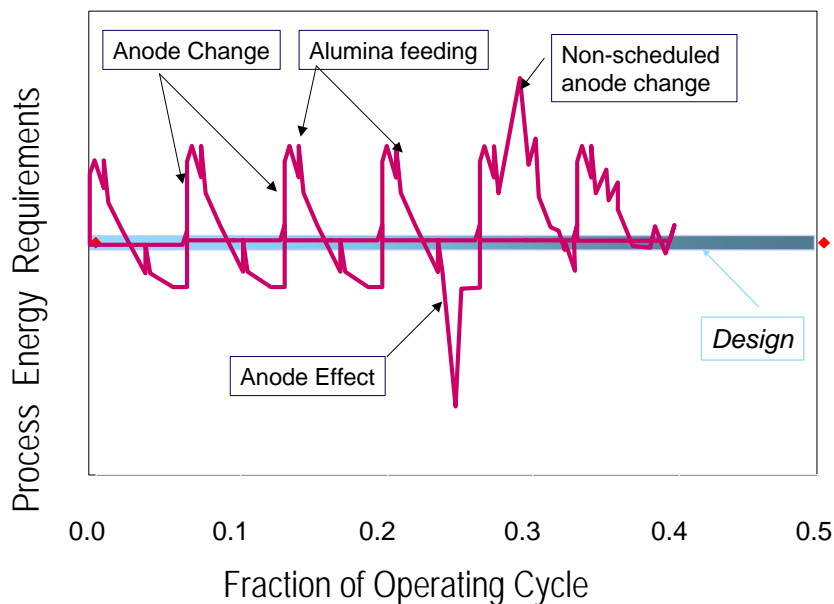

Figure 8: Change in energy balance over time (assuming constant setpoint voltage and amperage)

Figure 9 gives a measure of the range of superheats that have been observed in a potroom of operating cells. Low values result in very poor dissolution of the alumina. This poor dissolution can lead to an over-feeding and sludge formation and accumulation. These changes not only have consequential effects on the aluminium fluoride requirements, but also help maintain the superheat low, thus accentuating a bad condition. In addition, a reduction in superheat causes freezing in of the side ledge, impacting on the mass of liquid bath. In contrast, when the superheat is higher than the design value, melting of the side ledge occurs. This can, in extreme situations, lead to a total melting of the side freeze,

10

almost doubling the volume and mass of liquid electrolyte. These changes in bath mass have a consequential impact on the analysed aluminium fluoride concentration. Thus, process operations and transient cell conditions as a consequence of these dynamic effects impact both the true and apparent demand for aluminium fluoride and the control analysis measures
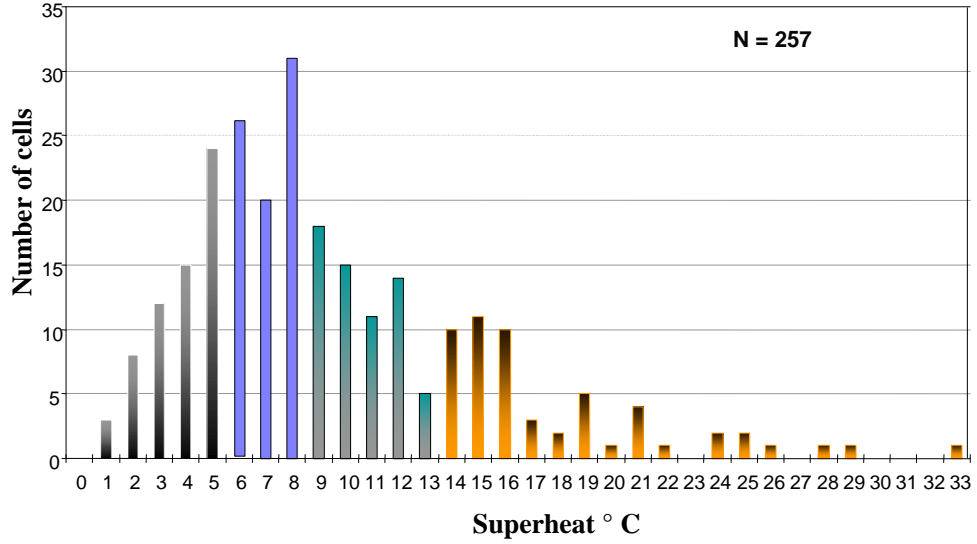

Figure 9: Superheat Variation in a Smelter

Aluminium Fluoride Control in Smelting Cells

The most common approach in determining the amount of aluminium fluoride to be added to a cell, is to modify a base amount in proportion to the deviations in analysed or measured process conditions – particularly the analysed aluminium fluoride concentration and/or the measured electrolyte temperature. Temperature is becoming a more common feature because it is more easily measured and can, therefore, have a quicker response characteristic. A typical general equation for aluminium fluoride control additions is as follows:

$$m_{AlF_3} = A + B(T_{bath\_actual} - T_{bath\_t\arg et}) + C(X_{AlF_3\_actual} - X_{AlF_3\_t\arg et})$$

This equation can take into account some of the base requirements within its cell constant (A). Usually either B or C equals zero, however some smelters incorporate both.

For smelters where C is zero, additions are adjusted on the basis of temperature alone. The temperature is used because, whilst frozen ledge exists, the temperature tends to track the phase diagram by the difference associated with the superheat. This however is based on the assumption that deviation from the target temperature is mainly due to changed aluminium fluoride concentration. In addition, the assumption often is made that the deviation in aluminium fluoride concentration is due to a deficit in the mass of aluminium fluoride in the bath. These assumptions can have limitations through reasons associated with variations in heat balance and process operations. For example, a change in temperature may only be partly due to a change in aluminium fluoride concentration. Changes in alumina concentration (impacting on liquidus temperature) or changes in superheat of the bath may be part of the cause, as illustrated by data in Table I. In addition, a change in aluminium fluoride concentration can be caused by a change in bath mass rather than changes in aluminium fluoride mass.

11

Table III: Percentage variation in temperature explained by variation in chemistry and superheat in a number of different cells
(Stevens McFadden 1998)

% variation in temperature explained by variation in:	Group X	Group Y	Group Z Time Period 1	Group Z Time Period 2
AlF$_3$	79	42	63	1
Al$_2$O$_3$	7	22	-23	30
Superheat	10	35	77	72

The limitations in this control approach is reflected by the process swings that are achieved in operating smelters (refer Figure 7) and the variability that inevitably result for different operations (refer Figures 9).

Causes for Variation in Temperature

Bath Temperature is equal to the liquidus temperature plus the superheat of the bath. Changes in the bath superheat or liquidus temperature will directly impact on bath temperature. Dynamic variation in liquidus temperature in industrial cells is predominantly due to changes in aluminium fluoride and alumina concentrations. Dynamic variation in superheat is caused by variation in the energy balance or by changes in parameters affecting heat loss from the cell, while this directly affects the bath temperature the more important effect comes indirectly, via the impact of variation in superheat on variation in bath mass via the ledge dynamics.

The transient changes in energy demand, associated with anode changing and alumina dissolution and changes in energy input due to anode effects, give rise to short term variation in superheat and freezing of electrolyte

The thermal impact of a new anode is concentrated in a localised zone in a cell. While the impact is technology and cell size dependent, some generalities can be drawn, as shown in Table IV. A new anode not only places a thermal demand on the electrolyte and metal pad, but it also leads to a redistribution of current with consequentially higher heat generation rates elsewhere. These impact last from 12 to 30 hours.

In contrast, the energy impact of an anode effect is more uniformly distributed. In some technologies anode effects last for only 30 seconds, others 200 seconds, and occasionally they may last several minutes. The intense heat generation rate results in a rapid increase in superheat, and thus a rapid melting of the side ledge. For prolonged AE's the side ledge has been shown to totally disappear (Taylor,1984 : Taylor and Welch, 1985).

Another transient and unpredictable thermal effect is the shorting ("spiking") of an anode to the metal pad. This typically results in a higher non-Faradic current through that anode generating the heat locally. While the impact of this can be accounted for in terms of current efficiency (see Table V), it will have the reverse impacts on superheat and electrolyte to that of a new anode within a cell.

Over-feeding and sludge formation occurs more slowly. While sludge build-up is occurring it is absorbing the pre-heat energy for the material, Whereas when sludge back-feeding is occurring, energy for dissolution is being absorbed. This tends to maintain the superheat at a low level during both the formation and dissolution of sludge.

**Table IV: Approximate changes (from steady state)
in cell superheat and ledge mass with process disturbances**

EVENT	LOCAL ZONE IN CELL		ELSEWHERE IN CELL	
	Superheat ($^{\circ}$C)	**Ledge Mass** (%)	**Superheat** ($^{\circ}$C)	**Ledge Mass** (%)
(a) Short Term* Impact*				
New Anode	-10 to -12	+50 to +90	-2 to 4	+20 to 40
Anode Spike	+3 to 6	-20 to -30	-1 to +2	-5 to +5
Anode Effect	+10 to +20	-50 to –100	+10 to +20	-50 to –100
(b) Long Term Impact**				
New Anode	-2 to –5	+20 to +50	-2 to –4	+20 to+40
Anode Spike	+3 to +6	-30 to –100	+1 to +3	-15 to -35
Anode Effect	+3 to +5	-30 to –90	+3 to +5	-30 to –90
* Short term approximately 0 to 2 hour time period ** Long term approximately greater than 6 hours				

In addition, medium term (day to day) changes in process parameters also impact on superheat, the freezing/melting of ledge and hence change bath mass. Predicted changes in superheat and ledge mass for given changes in process variables are detailed in Table IV. The changes considered are the largest change in process variables from their target levels that typically occur from one day to the next. This data is from steady state thermal modelling of a typical cell, note that changes in only one parameter is considered, in isolation of the secondary effects due to the resulting changes in other parameters that also affect the energy balance outcomes. For example, addition of voltage which causes the decrease in ledge mass and hence increase in bath mass, will also cause as a consequence, an increase in bath height, reduction in metal height and aluminium fluoride concentration and probably current efficiency. Some of these secondary changes have a reinforcing effect and others a balancing effect on the impact of the voltage on superheat and ledge mass. To determine the overall effect, significantly more sophisticated modelling would need to be performed, however the results do show that the impact of changes in process variables on superheat and ledge mass is significant.

Table V: Predicted changes (steady state) in cell superheat and ledge mass with the changes in process variables that can possibly occur from one day to the next.

Process Variable	Change	Impact On:	
		Superheat (^{o}C)	**Ledge Mass (% change)**
Cell Voltage	+250/-20mV	+2.9/-0.2	-30/+4
Amperage	+0.1/-2kA	+0/-0.3	-0/+6
Excess AlF3	+2/-3%	+0.3/-0.6	-4/+13
Alumina	+/-2%	+0.3/-0.6	-3/+12
Metal height	+/-20mm	-/+0.7	+/-10
Bath height	+/-30mm	-/+0.5	+/-17
Current efficiency	+/-4%	-/+0.8	+/-12

Given that the mass of ledge in a cell is typically the same as that of the bath (or in some instances more), these predicted changes in ledge mass will cause a similar or even greater percentage change in bath mass. A change of +/-20% in bath mass would cause a change in excess AlF$_3$ of +/-2wt% for cells with typical cell chemistries. Changes in excess AlF$_3$ of

this order (or +/-15°C of liquidus/bath temperature) can be observed from one day to the next. The data presented above suggests energy balance related changes in bath mass might be a likely explanation, rather than changes in the mass of AlF_3 in the bath due to changes in cell aluminium fluoride demand.

Accuracy of Measurements within the Cell and Reliability of Data

When the cell is sampled (for electrolyte composition), or conditions measured (for temperature), this is done at a fixed location in a cell. Often it is done at a fixed time in the work practice cycle. Thereafter it is assumed to be representative of the cell condition. However, Purdie (1992) has shown that not only is mixing within the cell a slow process, but also the temperature varies within the cell. The latter, illustrated in Figure 10, can vary by more than 10°C.

At least part of the spatial temperature variation is likely to be associated with the work practices discussed in the preceding sections of this manuscript.
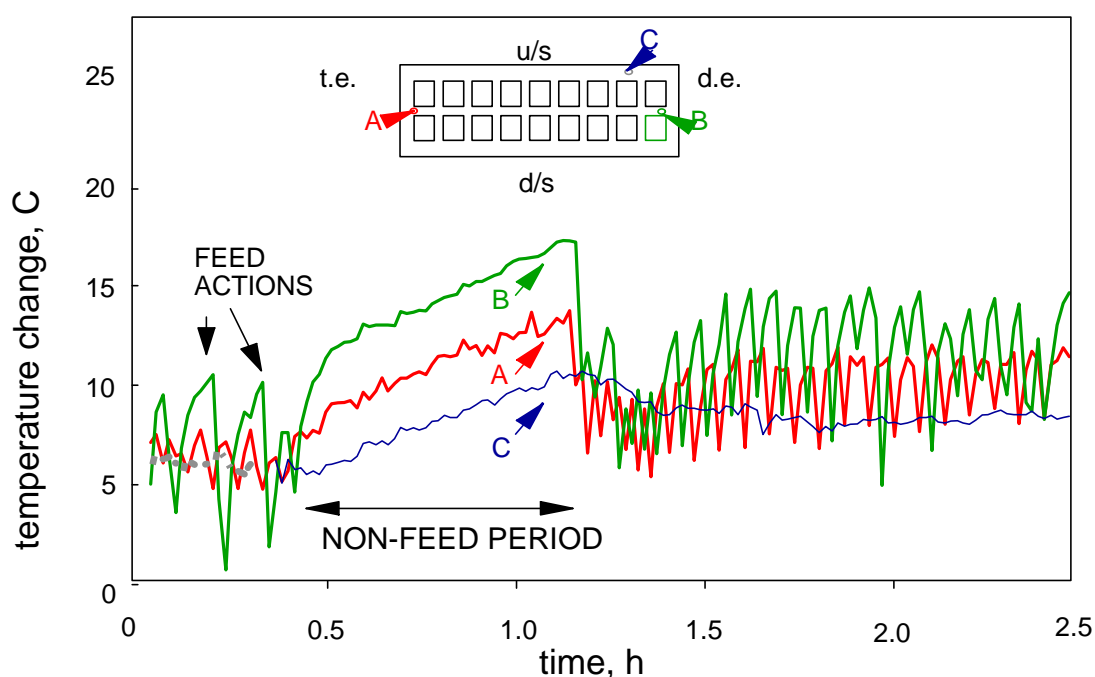

Figure 10: Variation in temperature at various locations in a cell

Spatial Variation in Temperature

Because of the potential impact of work practices on the local variation in temperature, a study has been made for several technologies on the impact of work practices on the measured temperature. Temperatures were measured at a fixed location on the cell and at a fixed time with respect to the work practices (that is, a prescribed time before metal tapping). If the variation in temperature observed was due to the anode change pattern and heat transfer, the magnitude of both the thermal effect and its resultant pattern would be dependent on the technology.

In order to determine this but eliminate local variations due to special conditions in the cell, the measured values of both aluminium fluoride concentration and temperature were analysed for ten randomly selected cells over three full anode change cycles. The data was averaged and compared against the average overall process conditions.
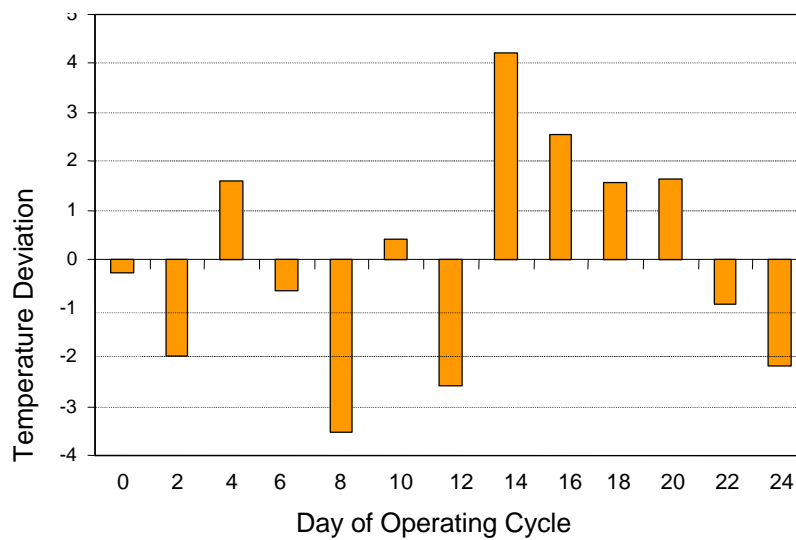
Figure 11: Average Temperature Deviation from target

Figure 11 presents the data obtained for one technology and it is seen that, depending on the day, there was a significant difference in the average temperature. The maximum differences occurred when anodes were changed most remotely from the measurement point in the cell. The resulting redistribution of the cell current, leads to a higher current density in the anodes near the measurement point, and hence a greater heating rate. Conversely, the lowest temperatures were recorded when the most recent anode changes occurred very near the measuring points. This trend was consistent for the two quite different anode setting patterns analysed.

Figure 12 illustrates the average aluminium fluoride additions associated with the same work cycle. As the smelter operates with a dry scrubber, the overall average should equate to that required for the sodium oxide content of the alumina, and this was the case. There is a similar cyclical behaviour of aluminium fluoride additions over the work cycle as that for temperature, which is expected given the control strategy in operation at this smelter. However, in this instance the data also shows that the addition rate is below that theoretically required when the cell is actually near its target condition early in the work cycle (eg on day zero). This under addition early in the work cycle is likely to accentuate the temperature behaviour associated with the work cycle and in addition mean that over-addition of aluminium fluoride is required in the later part of the work so that the average demand is satisfied
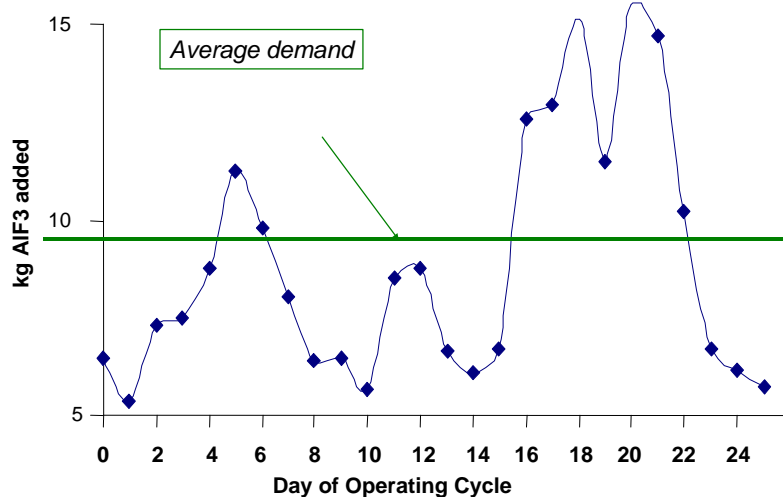

Figure 12: Aluminium Fluoride additions over the work cycle

Summary and Conclusions

The analysis of the aluminium fluoride demand has shown that from a materials balance viewpoint there is unlikely to be a significant change in the amount of aluminium fluoride required per day on the average. The concentration however, can vary dramatically on a daily basis through deviations in the energy balance from the target. This imbalance is

accentuated by spatial variation and hence measurement errors due to the condition being sensed in only one location in the cell. In summary:

1. Measured values of aluminium fluoride concentration and temperature are influenced spatially because of work practices.
2. The spatial variations can be characterised and understood from the anode setting practice.
3. Some process abnormalities (such as anode effects and extra cell voltage) lead to cell wide shifts in measurements whilst others (such as anode change and anode spike formation) lead to a more localised effect.
4. Because the average temperature and aluminium fluoride concentrations over the full work cycle tend to be on target, using the theoretical requirements is a good basis for maintenance of aluminium fluoride mass in the cell.
5. Apparent time constants and time lags encountered by some smelters after fluoride additions may in fact be explained due to the dynamic variability and pattern of work practices.
6. A weighted balance between the desire to maintain aluminium fluoride concentration and the need to have a global aluminium fluoride material balance may reduce the dynamics observed in the cell.
7. All aluminium fluoride maintenance programs should benefit by making allowance for the spatial variation in process measurements.

Whilst the energy imbalances of the cell are the root cause of variation in temperature, these imbalances usually arise from either work practices or cell abnormalities. The dynamic variations will account for work practices, but not the abnormalities. Thus, the long-term future control can best be addressed by better detection systems for cell abnormalities.

References
Haupin, W. and Kvande, H. (1993). "Mathematical Model of fluoride evolution from Hall Heroult cells". Light Metals 1993, pp 257 – 263.

Henry, J.L. (1963). "A study affecting fluoride emission from 10,000 ampere experimental Aluminium reduction cells". Extractive Metallurgy of Aluminium. Volume 2 – Aluminium. John Wiley and Sons. pp 67 – 81.

Hyland, M.M., Welch, B.J. and Metson, J.B. (2000). "Changing knowledge and practices towards minimising fluoride and sulphur emissions from aluminium reduction cells". Light Metals 2000, pp 333-338.

Stevens McFadden, F. J. (1998). "Energy Balance and Cell Dynamics: Considerations for Cell Design, Operations and Process Control". in Proc 6th Australasian Aluminium Smelting Conference and Workshop, (Eds M Skyllas-Kazacos & B J Welch) Queenstown, New Zealand, pp 289-320.

Taylor M.P. "The Influence of Process Dynamics on the Heat Balance and Cell Operation in the Electrowinning of Aluminium" PhD Thesis , University of Auckland (1984).

Taylor, MP and Welch, B.J., (1985) "Process Dynamics and Heat Balance - Implications for Operating Strategy, Control and Future Design". Incal-*85 (Ind.Inst.Met.)*, pp 85-98.

Taylor, MP, (1997) "Challenges in Optimising and Controlling the Electrolyte in Aluminium Smelters" in Proc 5th International Conference on Molten Slags, Fluxes and Salts (ISS) Sydney, January 1997, pp 659-674.

Welch, B.J. (1998) "Impact of Changes in Cell Heat Balance and Operations on the Electrolyte Composition" in Proc 6th Australasian Aluminium Smelting Conference and Workshop, (Eds M Skyllas-Kazacos & B J Welch) Queenstown, New Zealand, pp. 191-204, November 1998.

Purdie J.M. " Alumina behaviour and related process variations in aluminium smelting " PhD Thesis , University of Auckland (1993).